Change Detection by Fusion/Contextual Classification based on a Hybrid DSmT Model and ICM with Constraints

Azeddine Elhassouny[1] , Soufiane Idbraim[1] , Aissam Bekkari[1] , Driss Mammass[1]

[1]IRF-SIC Laboratory, Faculty of science, Agadir, Morocoo

Danielle Ducrot
CESBIO Laboratory
Toulouse. France

ABSTRACT
The Dezert - Smarandache Theory (DSmT) used for the fusion and the modeling of the classes sets of themes has shown its performances in the detection and the cartography of the changes. Moreover the contextual classification with the research for the optimal solution by an ICM (Iterated conditional mode) algorithm with constraints allows to take in account the parcellary aspect of the thematic classes, thus, the introduction of this contextual information in the fusion process has enabled us to better identify the topics of surface and the detection of the changes.

The objective of this work is, in the first place, the integration in a fusion process using hybrid DSmT model, both, the contextual information obtained from a supervised ICM classification with constraints and the temporal information with the use of two images taken at two different dates. Secondly, we have proposed a new decision rule based on the DSmP transformation to overcome the inherent limitations of the decision rules thus use the maximum of generalized belief functions. The approach is evaluated on two LANDSAT ETM+ images, the results are promising.

Keywords
Detection of the changes, Image classification, Fusion, Hybrid DSmT model, Decision rule, DSmP, Satellite images, ICM.

1. INTRODUCTION
The management and the follow-up of the rural areas evolution are one of the major concerns for country planning. The satellite images offer a rapid and economic access to accurate homogeneous and updated information of studied territories. An example of application which results from this is related to the topic of the changes cartography, in this paper, we are interested to study the most subtle changes of the Argan land cover and other themes in the region of Agadir (Morocco) by contextual fusion /classification multidates based on hybrid DSmT model [1-3] and ICM with constraints [4, 5].

Our work environment, is the theory of Dezert-Smarandache [1-3] which is recent and very little implemented or used before the covered work of this paper, it was applied in multidate fusion for the short-term prediction of the winter land cover [6-10] and, recently, for the fusion and the multidate classification [11-14], although the theory of evidence, it is more exploited for fusion/classification [11, 12, 15-20] also, for classifier fusion [21-23].

Our methodology can be summarized as following, after preprocessing of the images, a supervised ICM classification with constraints [4, 5] is applied to the two images, in order to recover the probabilities matrices for an after using in a step of fusion/classification basing on the theory of plausible and paradoxical reasoning known as Dezert-Smarandache Theory (DSmT) which allows to better assign the suitable pixels to the appropriate classes and also to detecte the changes.

The method is tested on two Landsat ETM+ images taken at two different dates corresponding to a good state of the vegetation and allows *a priori* an optimal response of the land cover. The validation with the test images have allowed better deducing the change sets of themes, thus the obtained results are clearly improved with the introduction of the spatial context (by ICM with constraints) into DSmT.

In this paper, in *section 2*, we describe in further detail the mathematical basis of the recent theory of plausible and paradoxical reasoning (DSmT), and give a description of our decision rule. The background and the details of the ICM algorithm with constraints are presented in *section 3*. In *section 4*, we provide the results of our experimentation where the algorithm was applied to a LANDSAT ETM+ image, the classification results are discussed in the same section followed by conclusions in *section 5*.

2. DEZERT SMARANDACHE THEORY (DSmT)

2.1 Principles of the DSmT
The DSm theory was conceived jointly by Jean Dezert and Florentin Smarandache[1-3], it is a new way of representing and fusioning uncertain information. DSmT, considered as a generalization of the evidence theory of Demspter-Shafer [15], was developed to overcome the inherent limitations of DST (Dempster-Shafer Theory) [1-3, 6-9, 13, 15, 24]. The basic idea of DSmT rests on the definition of the *hyper power set*, from which the mass functions, the combination rules and the generalized belief functions are built.

The *hyper power set* D^Θ is defined as the set of all composite propositions/subsets built from elements of Θ with $\cup$ and $\cap$ operators such as:

We define *hyper power set,* D^Θ as follow:

1. $\phi, \theta_1, \theta_2, ...\theta_n \in D^\Theta$

2. If $X, Y \in D^\Theta$, then $X \cup Y \in D^\Theta$ and $X \cap Y \in D^\Theta$.

3. No other elements belong to D^Θ, except those obtained by using rules (1) and (2) [1-3].

With $\Theta = \{\theta_1, \theta_2, ...\theta n\}, \phi$ is empty set.

We define a map as follows:

$$m_s(.) : D^\Theta \rightarrow [0,1] \quad (1)$$

Associated to a given body of evidence s as

$$m_s(\phi) = 0 \quad (2)$$

and

$$\sum_{X \in D^\Theta} m_s(X) = 1 \quad (3)$$

with $m_s(X)$ is called the generalized basic belief assignment/mass (gbba) of X made by the source s.

The DSmT contains two models : the free model and the hybrid model [1-3, 6, 7, 9, 11, 24], the first presents limits concerning the size of the *hyper power set* D^Θ, whereas the second has the advantage of minimizing this size, for this reason, it will be used in the continuation of our study.

2.2 Hybrid DSmT model

2.2.1 Hybrid DSmT model basis

It is easy to calculate the necessary memory size to the storage of the elements of D^Θ according to the cardinality n of Θ. Indeed, since each element of D^Θ can be represented by a binary word of $2^n - 1$ bits, the necessary memory size to storage D^Θ is given in the last column of the table 1, which shows an extreme difficulty for our actual calculators to be able to store D^Θ for dimensions $n > 6$.

Table 1. Cardinalities and necessary memory size for each *hyper power set*

Card(Θ)	Size(θ_i)	Card(D^Θ)	Memory(D^Θ)
2	1 byte	4	4 byte
3	1 byte	19	19 byte
4	2 byte	166	0.32 Kb
5	4 byte	7569	$\approx 30Kb$
6	8 byte	7828352	$\approx 59Mb$
7	16 byte	2414682040996	$\approx 3.6 \times 10^4 Gb$
8	32 byte	$\approx 5.6 \times 10^{11}$	$\approx 1.7 \times 10^{15} Gb$

A hybrid model is defined starting from the free model by introduction of different integrities constraints (exclusivity constraints, non-existential constraints or mixed constraints) [1-3, 6, 11] to some elements B of D^Θ, by forcing these elements to be empty in the new hybrid DSmT model $M(\Theta)$ and with the condition that we have knowledge of the study area or that we know the authentic nature of each of these elements in the studied problem. In our work, some exclusivity constraints are used to represent the non-adjacent elements of the study area like Argan (A) and Greenhouse (Gh).

2.2.2 Reduction of hyper power set D^Θ

Considering D_N, the generating matrix of *hyper power set* D^Θ, u_N the appropriate codification base of Smarandache, d_N the elements vector of D^Θ, d'_N the non-empty elements vector of D^Θ, u'_N the reduced codification vector of Smarandache associated to the hybrid DSmT model M' and D'_N a simplified binary matrix associated to M'.

If the constraint: an empty B unit of D^Θ is imposed (i.e. we choose a hybrid DSmT model), we eliminate in the matrix D_N the columns corresponding to the parts which compose B, the row of B and the rows of all the elements of D^Θ which are subsets of B, we obtain a new matrix D'_N representing a new hybrid DSmT model M'.

In the base u_N, we eliminate also the parts which form B, so, the dimension of this base becomes $2^N - 1 - C_M(B)$, with $C_M(B)$ indicates the cardinality of B in the hybrid DSmT model.

Any element α_i of D'_N can be obtained by the resolution of a simple linear equations system [1-3, 11]:

$$d'_N = D'_N \cdot u'_N \quad (4)$$

2.3 Combination rules

The masses from the sources must be combined using a combination rule to have a new masses distribution for the elements of the *hyper power set* in order to promote an item compared to others.

Within the framework of DSmT, there are several rules combination, for examples: Smets combinations rules, Dempster - Shafer (standardized) rule, Yager rule, disjunctive rule combination, Florea criterium, PCR5(Proportional Conflict Redistribution), Dubois and Prade (mixt rule combination), Martin and Osswald criterium (mixt rule combination,DPCR, MDPCR), the rule of Zhang and DSmH rule [1-3, 13]. In our application, we have applied and implemented the majority of these rules in order to choose those which allow us to have good performances such as the PCR5.

Mainly, the PCR5 rule is based on the principle of the (total or partial) conflicting masses redistribution [12] to the non-empty sets involved in the conflicts proportionally with respect to their masses assigned by the sources (it can be also generalized for $N > 2$ sources).

Considering the frame of discernment $\Theta = \{A, B\}$, two independent experts, and the two following bbas $m_1(.)$ and $m_2(.)$. The conflict induced by $m_1(A)$ and $m_2(B)$ is $m_1(A) \times m_2(B)$, this conflict grows the mass of the empty set and it is not taken in account when deciding, which is often done in DST. In DSmT, PCR5 rule redistributes the conflict [25], by adding

$m_1^2(X_1)m_2(X_2)/(m_1(X_1)+m_2(X_2))$ to $m_1(X_1)$

and

$m_2^2(X_1)m_1(X_2)/(m_1(X_1)+m_2(X_2))$ to $m_2(X_2)$.

The formula of PCR5 for $s > 2$ sources is given in [25].

2.4 Generalized belief functions

From the function of basic mass, the generalized belief functions (Credibility (Cr) , Plausibility (Pl) [1-3, 13, 25], $(DSmP)$ Transformation, $\cdots$ etc [3, 11, 26, 27]) are defined, which model the imprecision and the uncertainty according to the hypothesis considered by a given source.

The generalized belief functions used in this study namely the Credibility (Cr), Plausibility (Pl) and DSmP Transformation are defined for D^Θ in $[0,1]$ and are given respectively by: Belief, plausibility and DSmP of an element $X \in D^\Theta$:

$$Bel(X) = \sum_{\substack{v \subseteq X \\ v \in D^\Theta}} m(v) \tag{5}$$

$$Pl(X) = \sum_{\substack{v \cap X \neq \phi \\ v \in D^\Theta}} m(v) \tag{6}$$

$$\begin{cases} DSmP_\varepsilon(\phi) = 0 \\ \forall X \in G^\Theta \setminus \{\phi\}, DSmP_\varepsilon(X) = \\ \sum_{Z \subseteq X \cap Y} m(Z) + \varepsilon \cdot C(X \cap Y) \\ \sum \frac{C(Z)=1}{\sum_{\substack{Z \subseteq Y \\ C(Z)=1}} m(Z) + \varepsilon \cdot C(Y)} m(Y) \end{cases} \tag{7}$$

where $\varepsilon \geq 0$ is an adjustment parameter and D^Θ possibly reduced by the introduction of the integrity constraints of the hybrid DSmT model.

$C(X \cap Y)$ and $C(Y)$ respectively indicate the cardinalities of the $Y \cap X$ and Y.

2.5 Decision rule

The decisions after combinations could be taken from the generalized basic belief assignment/mass (gbba) or the generalized belief functions (Credibility (Cr), Plausibility (Pl), (DSmP) transformation $\cdots$ etc), thus, to decide the belonging of a pixel to a given class, two cases are distinguished:

• The pixel belonging to a simple class (used to improve a classification): in this case we use one of the following decision criteria: maximum of bba, maximum of the Credibility (Cr) (with or without rejection), maximum of the Plausibility (Pl), Appriou criterium, DSmP criterium $\cdots$ etc) [6, 7, 11, 13, 16].

• The pixel belonging to a composed class(e.g. in the case of change detection), in this case we cannot use the functions quoted previously because they are increasing functions and unsuited to the decision for the elements of union and of intersection.

In an original step, we have proposed a new decision rule based on DSmP transformation and confidence interval to take in account the composed classes. In this decision rule we exploited the confidence interval $[Bel(X), Pl(X)]$ by the definition of a new measurement which we have named: Global uncertainty $IncG$ which is the sum of the uncertainties (Inc) of the *hyper power set* elements:

$$\forall X \in D^\Theta \; Inc(X) = Pl(X) - Bel(X) \tag{8}$$

This new decision rule described in Algorithm 1 is applied as follows:

For a given pixel x, we compare the Global uncertainty $IncG$ of this pixel with a threshold (chosen experimentally). If it is lower than this threshold, the pixel is affected to the simple class which maximizes the DSmP transformation of all the simple classes, if not, it is affected to the composed class which maximizes the mass (bba) of all the composed classes.

The proposed decision rule

$IncG = \sum_{X \in D^\Theta} (Pl(x) - Bel(x))$

If $(IncG \le threshold)$ **then**

  If $DSmP[x](\theta_i) = max\{DSmP[x](\theta_i)$ $with\ 1 \le i \le n\}$ **then**

    $x \in \theta_i$

  End if

Else

  If $m[x](\cap \theta_i) = max\{m[x](\cap \theta_i)$ $with\ 1 \le i \le |D^\Theta| - (n+1)\}$ **then**

    $x \in \cap\theta_i$

  End if

End if

Other decision rules can be implemented based on our decision rule mentioned above by using Credibility (Cr) or Plausibility (Pl), $\cdots$ etc instead of DSmP.

2.6 Estimate of functions mass: Generalized Model of Appriou

The generalized model of Appriou [11, 12] is used to estimate the mass functions for the *hyper power set* elements, it can be described as follows: After the supervised ICM classification with constraints of the two images which generates the matrices of the probabilities $P(x_s/\theta_i)$ of pixels belonging to the simple classes $\theta_i (i = 1, \cdots, k)$ that form the frame of discernment Θ, a fusion rule of the masses is applied to combine all the masses affected by each source $S_i^b (i = 1, \cdots, k)$ to this element.

With:

- k is the number of classes.
- p is the number of sources.
- The element θ_i of Θ is considered as a source S_i^b .
- $S^b (b = 1, \cdots, p)$ is the source (satellite sensor or image).

The Appriou model for more than two classes is defined as follows:

$$\forall i = 1, \cdots, k;$$

$$m_i^b[x_s^b](\theta_i) = \frac{\alpha_i^b R^b P(x_s^b \mid \theta_i)}{1 + R^b P(x_s^b \mid \theta_i)} - \frac{|D^\theta| - k - 2}{k} \quad (9)$$

$$\forall i = 1, \cdots, k; r \ne i; k \ne i,$$

$$m_i^b[x_s^b](\theta_r) = \frac{\frac{\alpha_i^b}{k-1}}{1 + R^b P(x_s^b \mid \theta_i)} - \frac{|D^\theta| - k - 2}{k} \quad (10)$$

$$m_i^b[x_s^b](\theta_1 \cap \theta_2) = m_i^b[x_s^b](\theta_1 \cap \theta_3) = \cdots = m_i^b[x_s^b](\theta_1 \cap \cdots \cap \theta_{k-1}) = \varepsilon \quad (11)$$

$$m_i^b[x_s^b](\theta_1 \cup \theta_2) = m_i^b[x_s^b](\theta_1 \cup \theta_3) = \cdots = m_i^b[x_s^b](\theta_1 \cup \cdots \cup \theta_{k-1}) = \varepsilon \quad (12)$$

$$m_i^b[x_s^b](\Theta) = 1 - \alpha_i^b \quad (13)$$

where k is the number of the considered classes, ε is a sensitivity factor that weights the mass functions in order to have their sum over all the hypothesis equal to 1, $P(x_s^b \mid \theta_i)$ is the conditional probability, α_i^b is a coarsening factor, and R^b represents a normalization factor that is introduced in the axiomatic approach in order to respect the mass and the plausibility definitions, which is given by:

$$R^b = \frac{1}{max_{i=1,\cdots,k} P(x_s^b \mid \theta_i)} \quad (14)$$

This model is used in our study with $k = 5$ (number of classes) which are: Argan (A), Built/Oued (BO), Greenhouses (Gh), Vegetation (V) and Bare ground (Bg). $p = 2$ represents the number of used images (sources).

α is determined from the confusion matrix of ICM classification with constraints, and ε is taken equal to 0.0001.

3. ICM CLASSIFICATION WITH CONSTRAINTS

The information contained in a satellite image is usually in the form of homogeneous objects. Indeed, an image of rural areas often consists of large homogeneous parcels, and therefore, an acceptable classified image must respect this property. Thus, the use of Markov Random Fields (MRF) takes in account this property of the neighborhood influence of a pixel on it. and therefore insists on coherence between the class of a pixel and that of its neighbors. It is a powerful mathematical tool for regularizing the classification of the satellite images.

Moreover, the Markovien formalism constitutes a gateway to introduce a several constraints (spatial context, map of contours, temporal context, etc), for this reason, we have used the suggested method by [4, 5] as a method of classification in order to generate the probabilities for DSmT. This technique of classification provides, in addition to the constraint of regularization, a new constraint of segmentation so to refine the

classification. these contextual constraints are controlled by a parameter of temperature in an iterative algorithm of optimization ICM (Iterated Conditional Mode).

The used method of classification opts for a MAP (maximization of the a $posteriori$) solution approached by the ICM initialized with maximum likelihood (ML), because, given the big size of the treated images, this deterministic method proves being more interesting thanks to the convergence speed towards the solution.

We have a noted image y considered as a realization of a Markov Random Field Y . x is a realization of the classified image modeled as a MRF and X is the field of the labels. We seek the MAP solution that maximizes the posterior probability which can be written as,

$$x_{opt} = argmax_x \left[P(X = x/Y = y)\right] \quad (15)$$

which corresponds to seek the configuration that minimizes the following energy function.

$$x_{opt} = argmin_{x_s} \left[E(x/y)\right] \quad (16)$$

with

$$E(x/y) = \frac{1}{T} \times U(x_s) + f\left(y_s, \mu_{x_s}, \Sigma_{x_s}\right) \quad (17)$$

where each class i is defined by a mean vector μ and a covariance matrix Σ_i . The gray level y_S in a site s depends only to the label x_S in this site.

This expression integrates a term related to the introduced constraints (U) controlled by a parameter of temperature (T) and a term of attachment to data f .

3.1 Introduction of constraints

The formalism of Markov Random Fields makes it possible to introduce, in a flexible way, the constraints of spatial context through their modeling by some potential functions. The used method introduces two constraints, the first is that of the Potts model (regularization or smoothing constraint) and the second is that of the contour (segmentation) , these constraints will make it possible to minimize the posterior energy in the classification, with the possibility to modulate the importance that we want to give to either of these constraints. The energy function of the constraints, associated to a site of the image is expressed as follow:

$$U(x_s) = \sum_{allconstraints} U_{constraint}(x_s) \quad (18)$$

$$U(x_s) = U_{smooth}(x_s) + U_{contour}(x_s) \quad (19)$$

Two spatial constraints are introduced through the energy function: a constraint of regularization (smoothing) that operates in the neighborhood of the pixel and a constraint of contours that depends to contour of the pixel by segment.

Concerning the previous equation of energy $(eq.17)$, the originality here, is the variability of temperature. Over the iterations, the influence of some parameters and in particular the parameters of spatial context and segmentation will increase. This method refines the classification by re-estimating the statistics of the classes according to the previous iteration and by giving more and more importance to contextual information through the parameter of temperature T.

4. RESULT AND DISCUSSION

4.1 Methodology

Our methodology can be summarized as follows, after preprocessing of the images, we will apply a supervised ICM classification with constraints [4, 5], then a model of Appriou will be used to estimate the mass functions followed by a fusion of the masses matrices resulting from the hybrid DSmT model and the calculation of the generalized belief functions. Finally the new decision rule will be deployed.

4.2 Study area and used data

The study area is located in the region of Souss, it is in southern Morocco. Geologically, it is the alluvial basin of the Oued Souss, separated from the Sahara by the Anti-Atlas mountains. The natural vegetation in the Souss is savanna dominated by the Argan (Argania spinosa), a local endemic tree found nowhere else, part of the area is now a UNESCO Biosphere reserve to protect this unique habitat. Also, the region is the first aground zone of the country known by theses cultures under shelter (greenhouses), in particular the tomato and the flowers.

Today, the part of Souss in the Moroccan exports is 55 % of citrus fruits, 95 % of tomatoes and 70 % of the scoops (vegetables, fruits). So the region has a variety of ground covers which are close radiometrically.

The satellite images used in this study were taken respectively, in 19 March 2002 and 12 April 2005 by the Landsat ETM+, and are defined by the coordinates (Path 203, Row 39), they contain 8 bands with a resolution of 30 m per pixel for each band except the thermal band 6 and the panchromatic band 8, which have respectively the resolution of 120 m and 15 m.

Figure 1 shows a 3D visualization of the RGB composite (TM 3 - TM 2 - TM 1) with the use of the Digital Elevation Model (DEM) and the figure 2 shows RGB composite of the two used images.

The date of acquisition corresponds to a good state of the green vegetation and permits then an optimal response of covering vegetation. The study area is specified by a red rectangle.

Fig 1: 3D visualization of the RGB composite (TM 3 - TM 2 - TM 1) of the Landsat ETM+ image

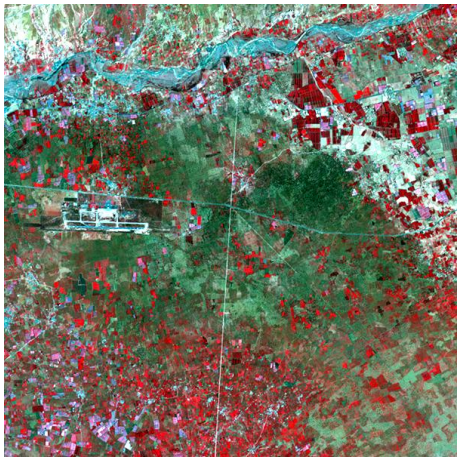

(a) Landsat ETM+ 2002

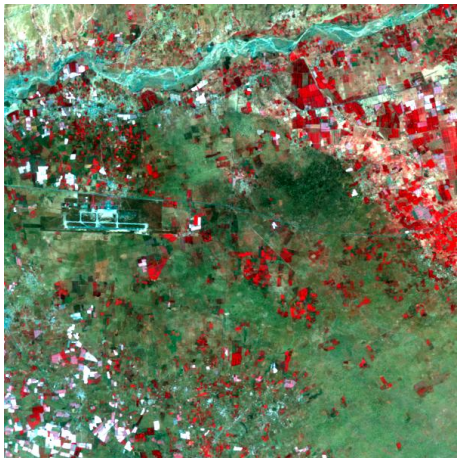

(b) Landsat ETM+ 2005

Fig 2: RGB composite of the Landsat ETM+ images 2002 and 2005 (Agadir, Morocoo)

4.3 Preprocessing of images

The preprocessing gathers the following processes: the sampling, the selection of the region of interest and the superposition of the images.

4.4 Trainings samples

The samples are created automatically by using the *ENVI* 4.0 software. We have identified 5 topics of land occupation: *Argan (A)*, *Built/Oued (BO)*, *Vegetation (V)*, *Greenhouses (Gh)* and *Bareground (Bg)* while basing on images already classified and on the ground truths.

The figure 3 (a) and figure 3 (b) represent the training samples used in ICM classification with contraintes established respectively for two images (ETM+ 2002 and ETM+ 2005), thus, figure 4 represents their spectral responses.

(a) Samples of Landsat ETM+ 2002

(b) Samples of Landsat ETM+ 2005]

Fig 3: Trainings samples of the images 2002 and 2005

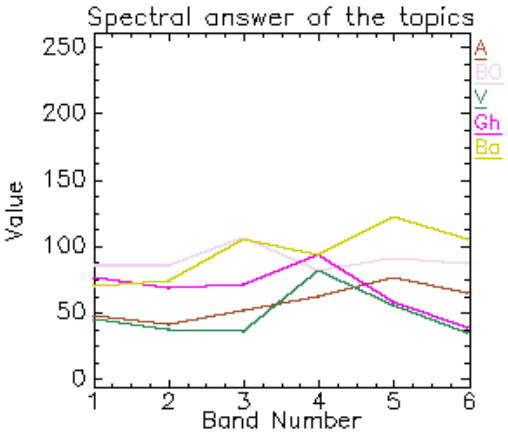

Fig 4: Spectral response of the topics

The number of pixels of training samples per class for the two images is shown in the following table 2.

Table 2. Training samples of the images 2002 and 2005

Class	Npixel02	Npixel05
Argan (A)	991	991
Built / Oued (BO)	245	245
Greenhouses (Gh)	144	343
Vegetation (V)	363	475
Bare ground (Bg)	286	433

4.5 ICM classification with constraints

After preprocessing of the two images and establishment of the samples, a supervised contextual ICM classification with constraints [4, 5] is applied to the two images to have the probabilities of pixels belonging to classes, which will be preserved in matrices (figure 5). The classified images are presented in figure 6.

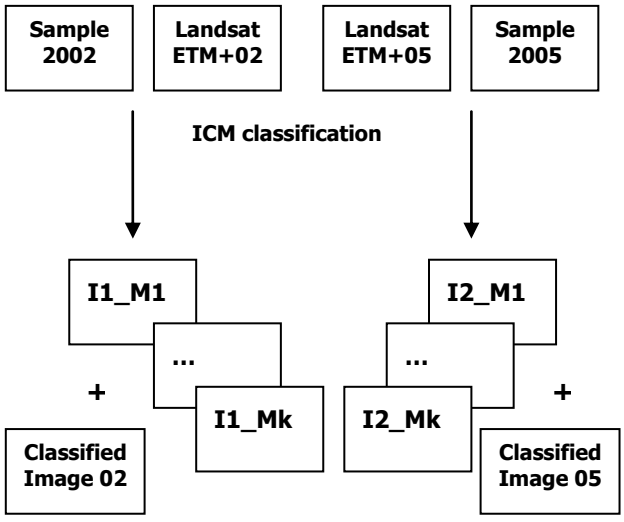

Fig 5: Diagram of Supervised ICM classification with constraints of the two images (Agadir, Morocco)

With

• Image 1:

- I1_M1: Contains the probabilities of the pixels belonging (image 1) to the class c1
- I1_M2: Contains the probabilities of the pixels belonging (image 1) to the class c2
- . . .
- I1_Mk: Contains the probabilities of the pixels belonging (image 1) to the class ck

• Image 2:

- I2_M1: Contains the probabilities of the pixels belonging (image 2) to the class c1
- I2_M2: Contains the probabilities of the pixels belonging (image 2) to the class c2
- . . .
- I2_Mk: Contains the probabilities of the pixels belonging (image 2) to the class ck

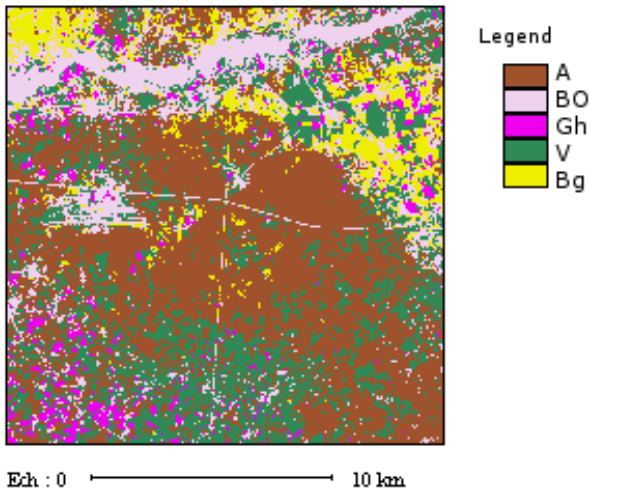

(a) ICM classification of Landsat ETM+ 2002

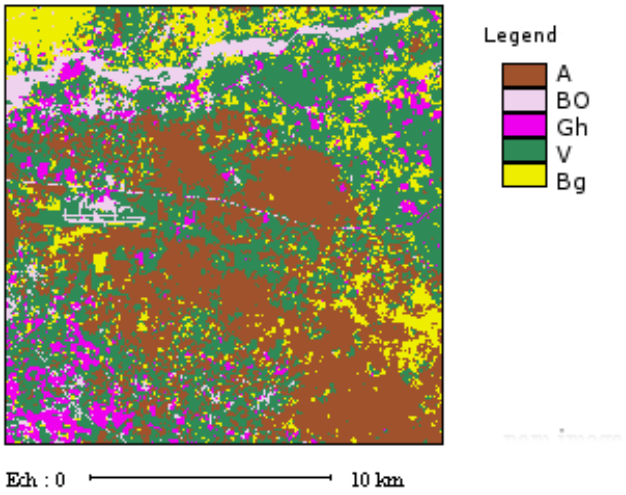

(b) ICM classification of Landsat ETM+ 2005

Fig 6: Supervised ICM classification with constraints of the two images (Agadir, Morocco)

By using the two resulting classified images, we generate a binary map of the changes shown in figure 7.

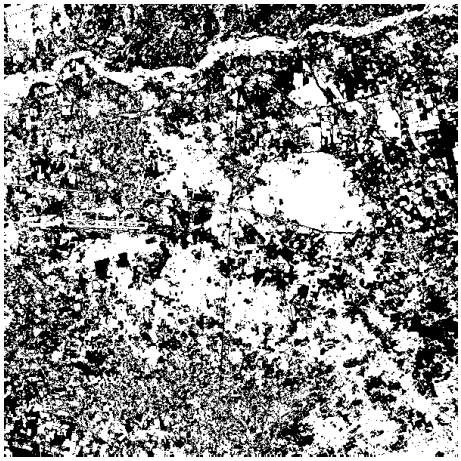

Fig 7: Binary changes map of ICM classification between 2002 and 2005 of the study area

4.6 Multidates and multi-source fusion by the hybrid DSmT model

Our fusion process is composed of the following steps, first the definition of the framework Θ, then, the estimation of the mass functions of each focal element by the model of Appriou, finally, the application of the hybrid DSmT model.

4.6.1 Hyper power set

Taking in consideration the prior knowledge of the study area, we have identified 5 classes constituting the framework Θ *section 4.4*, which are: *Argan (A), Built/Oued (BO), Vegetation (V), Greenhouses (Gh)* and Bareground *(Bg).*

So, Θ is defined as follows: $\Theta = \{A, BO, Gh, V, Bg\}$ Exploiting information of the study area and also those obtained by ICM classifications with constraints, some elements of the *hyper power set* D^{Θ} seem not being adjacents and exclusives. To realize a better adapted study to the real situations, some exclusivity constraints will be taken (hybrid DSmT model), for example $A \cap Gh = \phi$, which reduces the number of focal elements of the D^{Θ}.

4.6.2 Choice of threshold

The decision is made for the simple classes and the classes of intersection by using our rule decision defined previously (*section2.5*), the threshold should be determined in advance by experimentation and analysis of total uncertainty distribution after standardization, wich is presented in figure 8.

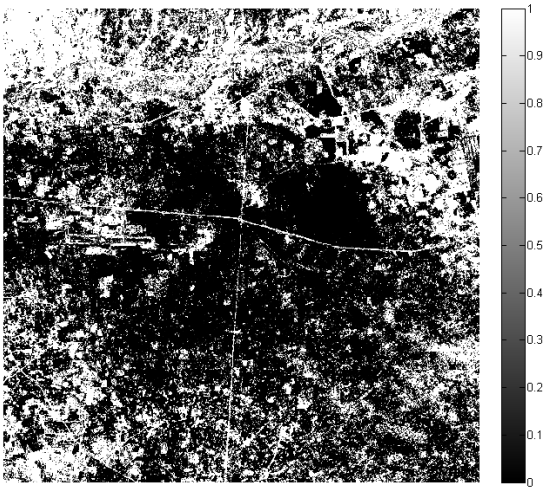

Fig 8: The standardized global uncertainty distribution of the fusion map

We have tested our decision rule with various values of threshold, the following table 3 presents the occupancy rates of the simple classes (stable zones) and composed classes (change zones) according to the threshold.

Table 3: Occupancy rates of the simple classes and the composed classes according to the value of the threshold

value of the threshold	(%)of stable zones	(%)of change zones
1.0e-26	0%	100%
1.0e-019	9.64%	90.36%
1.0e-016	32.12%	67.88%
1.0e-014	54.408%	45.592%
1.0e-012	76.86%	23.32%
1.0e-08	99.99	%0.01%

The choice of threshold depends to the good results of detection with the use of the changed/ unchanged samples between the two dates (2002 and 2005), for this we have taken a suitable threshold that equal to $1.0e^{-14}$.

4.6.3 Result of fusion/classification according to threshold

In figure 9 below, the result of contextual multi-source multidates fusion/classification of LANDSAT ETM+ images by using the combination rule PCR5 and our decision rule with different thresholds.

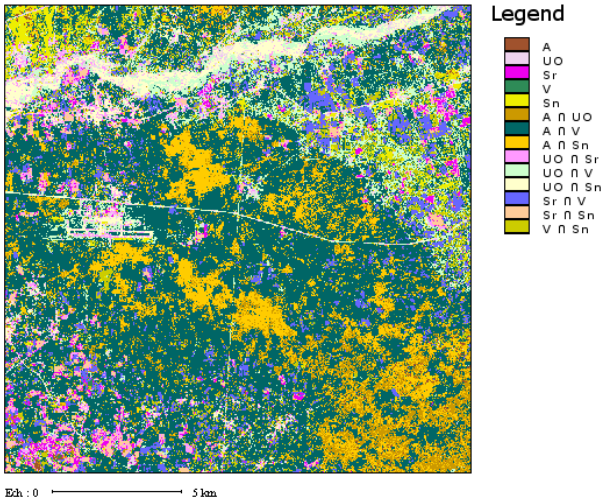

(a) Threshold=(1.0e-19)

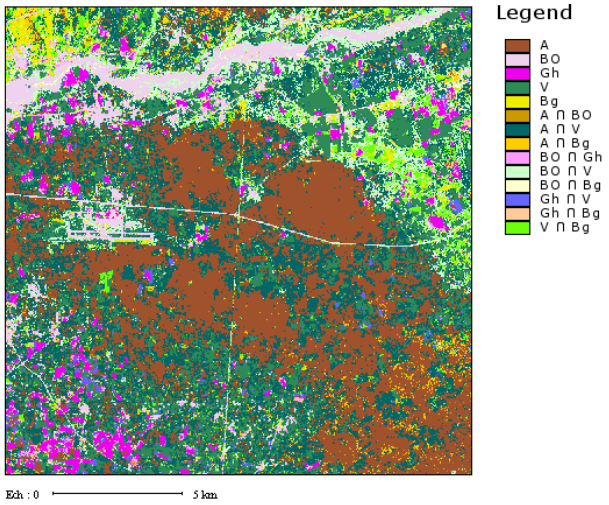

(b) Threshold=(1.0e-14)

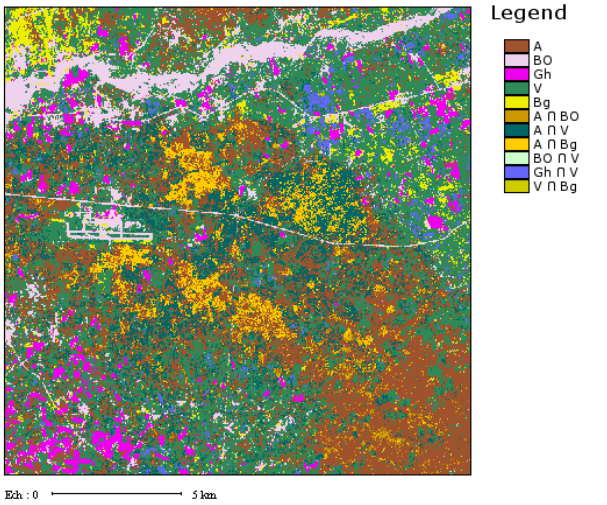

(c) Threshold= (1.0e-12)

Fig 9: Result of fusion/classification according to threshold

The results obtained with the various values of the threshold are as follows: a map contains 100% of the composed classes for the threshold of $1.0e-26$, 0.01% for the threshold of $1.0e-8$ and 45.592% for the threshold of $1.0e-14$. The first result does not match with the ground truths because several areas of the region are unchanged during the considered period. The second result is far from the dynamic reality of the region that has known a great change. The last result is coherent and appears to be close to reality basing on the test samples of the stable zones and the zones of changes between the two images, while for thresholds which exceed the surrounding of $(1.0e-14)$ there is a degradation of the change detection

4.6.4 Validation of the results

The fusion map obtained with an adequate threshold = (1.0e-14) is presented in figure 10.

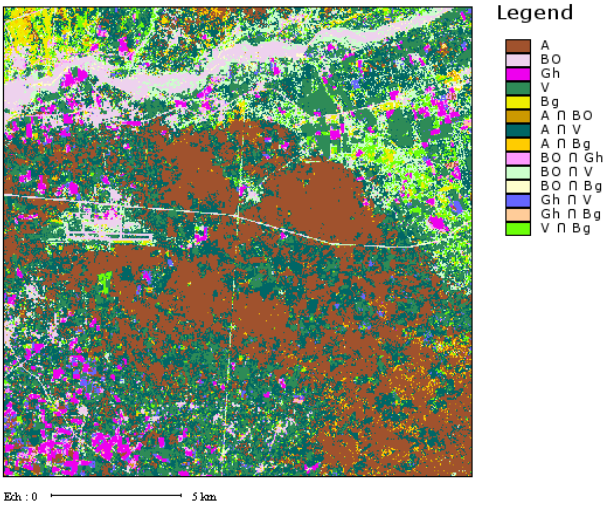

Fig 10: Fusion map obtained with threshold of (1.0e-14)

From the fusion map, obtained with an adequate threshold we obtain the table 4 presenting the occupancy rate of the classes.

Table 4. Occupancy rate of the classes

Class	(%)
A	29.04%
BO	4.869%
Gh	3.18%
V	15.92%
Bg	1.399%
A ∩ BO	0.649%
A ∩ V	26.40%
A ∩ Bg	1.87%
BO ∩ Gh	1.549%
BO ∩ V	7.25%
BO ∩ Bg	1.08%
Gh ∩ V	1.98%
Gh ∩ Bg	0.5%
V ∩ Bg	3.30`%

The table 4 illustrates the occupancy rates of the stable zones (simple classes) which reaches the rate of 54.408% and that of the zones of change (composed classes) which reaches 45.592%. From the table 4, we note that the Argan class (A) and Vegetation class (V) have known a great change compared to the other classes, indeed, we found for the composed class $(A \cap V)$ a rate of change of 26.40%.

Other classes have also known changes, especially the Built / Oued class (BO) , the Bare ground class (Bg) and the Greenhouses class (Gh) wich are found respectively in the composed class $(BO \cap V)$ with a rate of 7.25%, in the composed class $(V \cap Bg)$ with a rate of 3.3% and in the composed class $(Gh \cap V)$ with a rate of 1.98%.

The figure 11 presents the stable zones map obtained from the fusion map.

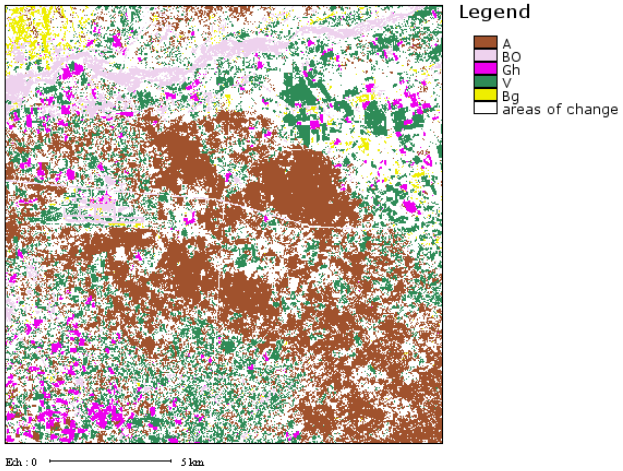

Fig 11: Stable zones map

From the stable zones map, we note that the zone of Oued Souss (BO), the zone of the urban areas along the road Agadir-Taroudant (BO), the international airport of Almassira (BO), the parcels of the Ouled teima region (V), the greenhouses (Gh) of the Biogra region and also some surface of argan (A) are all well detected as stable zones and are assigned to simple classes. This attribution is well justified because some zones are built and are unchangeable by nature.

For the change zones, figure 12 and figure 13 illustrate those zones obtained from the fusion map.

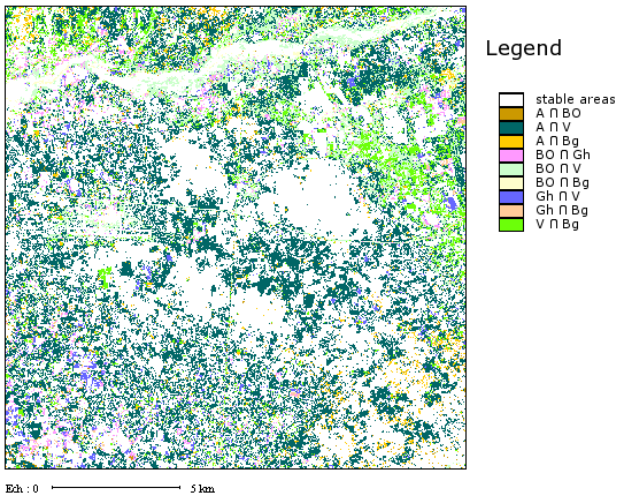

Fig 12: Change zones map obtained from fusion map

Areas that have known major changes are the Argan class wich becomes bare ground or vegetation, which is well explained because of the deforestation.

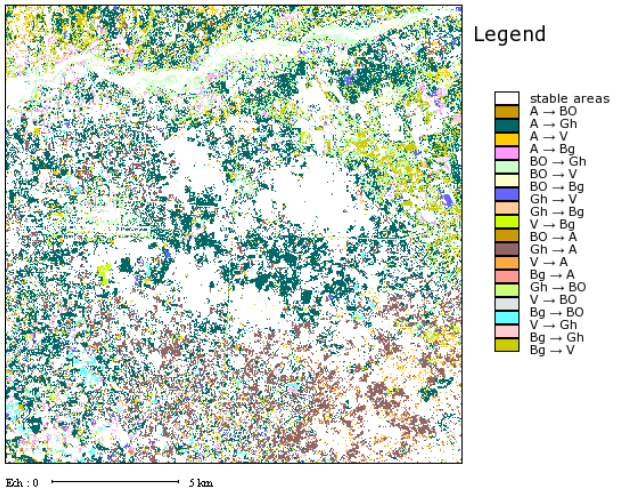

Fig 13: Post-processed map of change zones obtained from fusion map

In the post-processed fusion map, we found a rate of 18.95 of the Argan class changed to vegetation in 2005. Also, there is the emergence of the greenhouses parcels in the 2005 image (which were in 2002, vegetation or bare ground) or, conversely, areas of greenhouses in 2002, are became in 2005 areas of vegetation or bare ground with a rate of change of 1.48%.

For inter-city roads, they are detected as a change class between Urban / Oued and Vegetation, which is well justified because the pixels of the roads in the image 2002 are covered by the pixels of Urban / Oued class, on the contrary, in the image 2005 (taken at a date corresponding to a good state of vegetation), they are covered by the pixels of the vegetation class which explains the belonging of those pixels to the composed class.

4.6.4.1 Validation per spectral signature of the results

To evaluate our proposed method, we have chosen to use spectral signatures of classes (themes) for the two images. For pixels of change areas , we have a variation in the spectral signature of the image pixels between 2002 and 2005. Conversely, the pixels of the stable areas have shown a stability of spectral signature between the two dates.

For this spectral evaluation, we have used the zoom window of the *ENVI* 4.0 software for the images ETM+ 2002, ETM+ 2005 and the fusion map to link them for locating the change zones in the fusion map (figure 12), Then we have compared the spectral signatures of the same area for the two images by taking in account the distributions of spectral signatures of different themes.

The following figures 14, 15, 16 present the extracts of validation of the change results.

(a) ETM+ 2002 (b) ETM+ 2005 (c) Fusion map

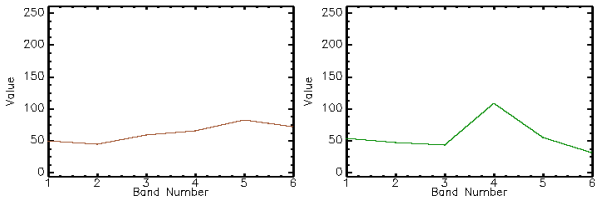

(e) Spectral signature of V (ETM+ 2002) (d) Spectral signature of A (ETM+ 2005)

Fig 14: Spectral signature of the Argan class (A) (ETM+2002) and of the Vegetation class (V) (ETM+ 2005)

From the figure 14, we note that the extract area has known a change of Argan theme (Class A) to vegetation theme (class V), what is shown by the change of the pixels spectral signature of the extract area which had in 2002 a spectral signature of the Argan (Class A), and became in 2005 that of the vegetation (Class V).

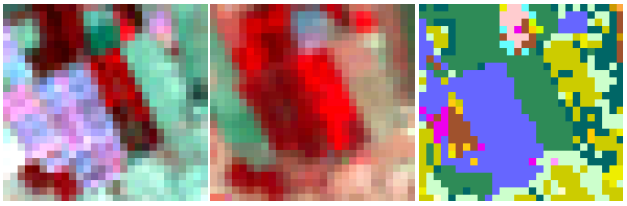

(a) ETM+ 2002 (b) ETM+ 2005 (c) Fusion map

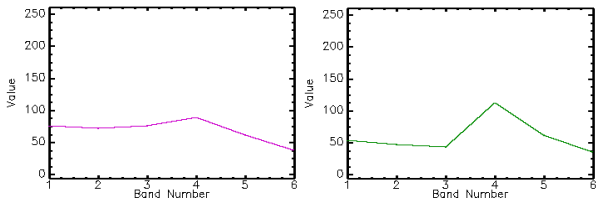

(e) Spectral signature of Gh (ETM+ 2002) (d) Spectral signature of V (ETM+ 2005)

Fig 15: Spectral signature of the Greenhouses class (Gh) (ETM+ 2002) and of the Vegetation class (V) (ETM+ 2005)

The figure 15 illustrates a change between Greenhouses class (Gh) and Vegetation class (V), as described before, the change is showed by the variation of spectral signature of the pixels between that of the Greenhouses theme (class Gh) in 2002 and that of the Vegetation theme (class V) in 2005.

(a) ETM+ 2002 (b) ETM+ 2005 (c) Fusion map

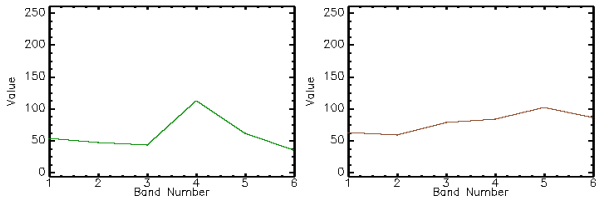

(e) Spectral signature of V (ETM+ 2002) (d) Spectral signature of A (ETM+ 2005)

Fig 16: Spectral signature of the Vegetation class (V) (ETM+ 2002) and of the Argan class (A) (ETM+ 2005)

Similarly, the figure 16 shows a change zone that was occupied by the vegetation (class V) in 2002 and became occupied by Argan (class A) in 2005. The spectral change signatures justify the affectation of pixels to the composed class $(V \cap A)$.

The table 5 illustrates the detection of the change by fusion

Table 5. Rate of change obtained by fusion between LANDSAT ETM+ 2002 and ETM+ 2005

Class	Number of pixels	Occupancy rate (%)
A	104,542	29.0394
BO	17,538	4.8717
GH	11,458	3.1828

V	57,320	15.9222
Bg	5,048	1.4022
A→ BO	797	0.2214
A→ V	68,202	18.9450
A →Bg	4,295	1.1931
BO→ Gh	4,650	1.2917
BO→ V	25,587	7.1075
BO Bg	3,227	0.8964
Gh→ V	3,112	0.8644
Gh→ Bg	471	0.1308
V→ Bg	2,662	0.7394
V→ A	26,889	7.4692
Bg→ A	2,439	0.6775
Gh→ BO	915	0.2542
V→ BO	502	0.1394
Bg→ BO	647	0.1797
V→ Gh	4,005	1.1125
Bg→ Gh	1,324	0.3678
Bg→ V	12,831	3.5642

With Argan (A), Built/Oued (BO), Greenhouses (Gh), Vegetation (V), Bare ground (Bg).

The figure 17 shows the post-processed map of the fusion.

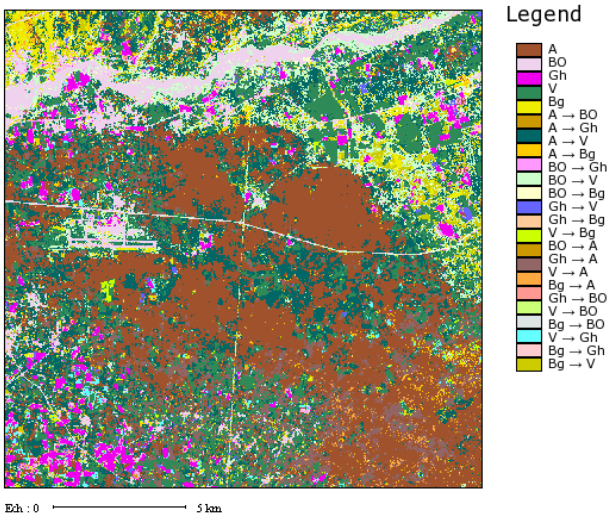

Fig 17: Post-processed fusion map

5. CONCLUSION

In this paper we have proposed a new method for land cover changes detection. In first, we have included the spatial information in the process of fusion/classification by using a hybrid DSmT model with the introduction of contextual information using ICM classification with constraints, the use jointly of DSmT and ICM improves performance of the changes detection in terms of accuracy and exactitude. Secondly, we have proposed a new decision rule that has shown its performance and allowed us to overcome the limitations of rules decision based on the maximum generalized belief functions which are increasing and unsuited to the decision of the union and the intersection of elements.

The application of this method for the catography of the land cover changes is promising, however, the determination of the adequate decision rule (currently we work on a dynamic fusion method) and the addition of a temporal constraint to allow the processing of different dates are still significant issues for further investigation.

6. ACKNOWLEDGMENTS

This work was funded by CNRST Morocco and CNRS France Grant under Convention CNRST CRNS program SPI09/11.

7. REFERENCES

[1] Smarandache, F. and Dezert J. (Editors). 2004. Advances and Applications of DSmT for Information Fusion (Collected works), vol. 1, American Research Press, Rehoboth, U.S.A.

[2] Smarandache, F. and Dezert, J. 2006. Advances and Applications of DSmT for Information Fusion (Collected works), vol. 2, American Research Press, Rehoboth, U.S.A.

[3] Smarandache, F. and Dezert, J. 2009. Applications and Advances of DSmT for Information Fusion (Collected works), Vol. 3, American Research Press, Rehoboth, ARP.

[4] Idbraim, S., Ducrot, D. D. Mammass and Aboutajdine, D. 2009. An unsupervised classification using a novel ICM method with constraints for land cover mapping from remote sensing imagery, International Review on Computers and Software (I.RE.CO.S.), Vol. 4, no. 2.

[5] Ducrot, D. 2005. Méthodes d'analyse et d'interprétation d'images de télédétection multi-sources Extraction de caractéristiques du paysage, habilitation thesis, France.

[6] Mercier, G.2007. Outils pour la télédétection opérationnelle, habilitation thesis, Rennes I university, France.

[7] Corgne, S., Hubert-Moy, L., Dezert, J. and Mercier, G. 2003. Land cover change prediction with a new theory of plausible and paradoxical reasoning, ISIF2003, Colorado, USA, March 2003.

[8] Smarandache, F. and Dezert, J. 2006. An Introduction to the DSm Theory for the Combination of Paradoxical, Uncertain and Imprecise Sources of Information, Information&Security International Journal, 1st August 2006.

[9] Moraa, B., Fourniera, R. A. and Foucherb, S. 2010. Application of evidential reasoning to improve the mapping of regenerating foreststands, International Journal of Applied Earth Observation and Geoinformation.

[10] Basse, R. M. 2006. Université de Nice, La prise en compte de l'incertitude dans une démarche de modélisation prédictive, MoDyS, Lyon, France, 8 and 9 Novembre 2006.

[11] Bouakache, A. and Belhadj-Aissa, A. 2009. Satellite image fusion using Dezert-Smarandache theory, DSmT-book3, Master Project Graduation, University Houari Boumediene.

[12] Khedam, R., Bouakache, A., Mercier, G. and Belhadj-Aissa, A. 2006. Fusion multidate à l'aide de la théorie de Dempster-Shafer pour la détection et la

cartographie des changements : application aux milieux urbain et périurbain de la région d'Alger, Télédétection, Vol. 6, no. 4, pp. 359 404.

[13] Djiknavorian, P. 2008. Fusion d'informations dans un cadre de raisonnement de Dezert-Smarandache appliquée sur des rapports de capteurs ESM sous le STANAG 1241, Memory to obtain the degree (M.Se.), Laval University, Quebec.

[14] Anne-Laure, J., Martin, A. and Maupin, P. 2008. Gestion de l'information paradoxale contrainte par des requêtes pour la classification de cibles dans un réseau de capteurs multi-modalités, SCIGRAD'08, Brest, France, 24-25 novembre 2008.

[15] Foucher, S., Germain, M., Boucher, J. M. and Bénié, G. B. 2002. Multisource Classification Using ICM and Dempster-Shafer Theory, IEEE Transaction on Instrumentation and Measurement, Vol. 51, no. 2, APRIL

[16] Bloch, I. 2003. Fusion d'informations en traitement du signal et des images, IC2, Hermès Science, Traité IC2, Paris, France.

[17] Bloch, I. Fusion d'informations en image et vision, ENST - CNRS UMR 5141 LTCI, Paris - France.

[18] Lemeret, Y., Lefevre, E. and Jolly, D. 2004. Fusion de données provenant d'un laser et d'un radar en utilisant la théorie de Dempster-Shafer, MAJECSTIC'04, France.

[19] Fiche, A. and Martin, A. 2009. Bayesian approach and continuous belief functions for classification, LFA, Annecy, France, 5-6 November 2009.

[20] Germain, M., Boucher, J. M., Bénié, G. B. and Beaudry, E. 2004. Fusion évidentielle multi source basée sur une nouvelle approche statistique floue, ISIVC04, Brest, France.

[21] Martin, A. 2005. Fusion de classifieurs pour la classification d'images sonar, RNTI-E-5, pp 259 268, novembre 2005.

[22] Chitoub, S. 2004. Combinaison de classifieurs : une approche pour l'amélioration de la classification d'images multisources multidates de télédétection, Télédétection, vol. 4, no. 3, pp. 289 301.

[23] Sitraka, R., Solofoarisoa, R. And Solofo, R. 2009. Combinaison de classificateurs selon la théorie de Dempster -Shafer pour la classification d'images satellitaires, Mada-Géo13 (ISSN 2074 4587), Mai 2009.

[24] Corgne, S. 2004. Modélisation prédictive de l'occupation des sols en contexte agricole intensif : application à la couverture hivernale des sols en Bretagne, Doctoral thesis, Rennes 2 university, france, 10 December 2004.

[25] Osswald, C. 2005. Modèles et consensus en fusion : influence sur la décision et la complexité du processus, seminar, ENSTA E^3I^2, France, 20 October 2005.

[26] Zhun-ga, L., Dezert, J. and Pan, Q. 2010. A new measure of dissimilarity between two basic belief assignments, hal-00488045, ScientificCommons, 1 Jun 2010.

[27] Dezert, J. and Smarandache, F. 2008. A new probabilistic transformation of belief mass assignment, International Conference on Information Fusion, Cologne: Germany (2008).